

## Optimization of Cutoff Energy and K-Point Grid Parameters for DFT Study of Pristine and Mg-Doped Silicene



\*<sup>1</sup>Onuik Princewill Chinagorom, <sup>1</sup>Tijjani Auwalu Musa,  
<sup>2,3</sup>Fagbenro Abiodun Bamidele and <sup>3</sup>Isiogu Ekene Chukwuma

<sup>1</sup>Department of Physics, Abubakar Tafawa Balewa University (ATBU), Bauchi State, Nigeria.

<sup>2</sup>Department of Physics, Ignatius Ajuru University of Education, Rumuolumeni, Port Harcourt, River State, Nigeria.

<sup>3</sup>Alvan Ikoku Federal University of Education, Owerri, Imo State, Nigeria.

\*Corresponding author's email: [onuikprincewill@gmail.com](mailto:onuikprincewill@gmail.com)

### ABSTRACT

Silicene, a two-dimensional material analogous to graphene, has garnered significant interest due to its promising applications in nanoelectronics, spintronics, and optoelectronics. Doping silicene with foreign atoms, such as magnesium (Mg), can modify its properties, enhancing stability and electronic versatility. This study investigates the optimization of computational parameters for pristine and Mg-doped silicene using Density Functional Theory (DFT) simulations within the Quantum ESPRESSO framework. The convergence behavior of the plane-wave cutoff energy ( $E_{cutwfc}$ ) and k-point grids was analyzed at doping concentrations of 3.125%, 6.25%, 12.5%, and 25% Mg. Results reveal that the optimal  $E_{cutwfc}$  values increase with higher doping concentrations, ranging from 60 Ry for pristine silicene to 200 Ry for 3.125% Mg doping. K-point grid analysis indicates that lower doping concentrations require relatively coarse grids, while higher concentrations demand finer grids for accurate results. This study provides a reference framework for parameter selection in doped silicene systems, offering valuable insights for future theoretical research and practical applications in the field of 2D materials.

### Keywords:

Cutoff-Energy,  
K-point,  
Silicene,  
DFT,  
Total Energy.

### INTRODUCTION

A 2D allotrope of silicon named silicene, exhibiting a honeycomb lattice structure similar to graphene, is establishing itself in electronics applications (Ornes, 2014). Due to its intrinsic properties, such as high carrier mobility, quantum spin Hall effect, and the potential for a tuneable bandgap, silicene holds significant promise for applications in nanoelectronics, spintronics, and optoelectronics (Zhao et al., 2016). However, silicene's low chemical stability and limited electronic versatility in its pristine form necessitate chemical modifications, such as adsorption (Feng et al., 2014), absorption (Chowdhury, 2016), and doping (Cocolezzi et al., 2017), to modify its properties. Magnesium (Mg) adsorption has been identified as a particularly effective method to enhance silicene's conductivity, stability, and electronic characteristics (Tran et al., 2020), making it a strong candidate for applications in energy storage field-effect transistors and photodetectors (Galashev, 2024).

In computational materials science, the plane-wave basis set and k-point grid are crucial parameters for accurately modelling the electronic structure of periodic systems. Cutoff energy ( $E_{cutwfc}$ ) defines the plane-wave basis set, which determines the maximum kinetic energy of the plane waves included in the calculations (François, 2023). The k-point grid determines the precision of sampling in the Brillouin zone, which is essential for capturing the material's electronic properties (Babbush et al., 2017). Density functional theory (DFT) calculations are essential for achieving correct predictions of these parameters, both fundamentally and technologically (Gheshlagh et al., 2020). Incorrect or non-converged values for these parameters will lead to inaccurate results of such critical material properties as band gap, Density of States (DoS) and total energy that may result in incorrect theoretical predictions, thereby misleading experimental endeavour (Tran et al., 2017). Optimizing these parameters requires a careful balance between computational performance and numerical precision. Too strict values

raise computing expenses needlessly, while values not adequately converged can cause significant inaccuracies in anticipated results (Sun et al., 2018).

This paper presents a detailed investigation into optimizing  $E_{\text{cutwfc}}$  and k-point mesh for Mg-doped silicene, where magnesium atoms are used to replace atoms of silicene at different percentages using DFT within the generalized gradient approximation (GGA). Total energy as a function of  $E_{\text{cutwfc}}$  and k-point density are essential properties whose convergence behaviour is methodically examined in this study. Its goal is to determine the ideal computational settings to create a benchmark framework for further theoretical investigations on doped silicene systems. Moreover, the outcomes will offer significant perspectives to direct researchers in fine-tuning magnesium-doped silicene for practical uses.

### MATERIALS AND METHODS

The optimization was carried out using the open-source DFT package Quantum ESPRESSO (QE) (Giannozzi et al., 2009) (Giannozzi et al., 2017) (Giannozzi et al., 2020). The input file for these simulations contains several essential components, including code calculations, data structure, parameter data, k-points, and pseudopotential files (Prandini, 2018). The `pw.x`

module within QE was used to perform the calculations. The Van der Waals (vdW) exchange-correlation (XC) (vdw-DF2-C09) (Thonhauser et al., 2007) (Thonhauser et al., 2015) (Berland et al., 2015) (Langreth et al., 2009) was used as the method for describing the interactions between electrons in the systems. The electronic interactions for Silicene and Magnesium were described using a norm-conserving pseudopotential obtained from the PSLibrary (Dal Corso, 2014). Relativistic effects were neglected, consistent with the non-relativistic nature of the pseudopotential.

In this study, the Mg-Doped Silicene system is obtained by doping different magnesium concentrations in the silicene lattice. Since the applications of the different doping levels are distinct and their substitutions modify electrical and mechanical properties (Galashev et al., 2023), specific parameters must be optimized to represent the material system behaviour properly; of these parameters, the kinetic energy cut-offs ( $E_{\text{cutwfc}}$ ) and k-point sampling need to be carefully optimized. The calculations were done for Mg content varied across doping levels of 3.125% (Mg:Si 1:32), 6.25% (Mg:Si 1:16), 12.5% (Mg:Si 2:16), and 25% (Mg:Si 4:16) as shown in fig.1(a-e). The convergence for pristine silicene was also calculated for comparison and reference purposes.

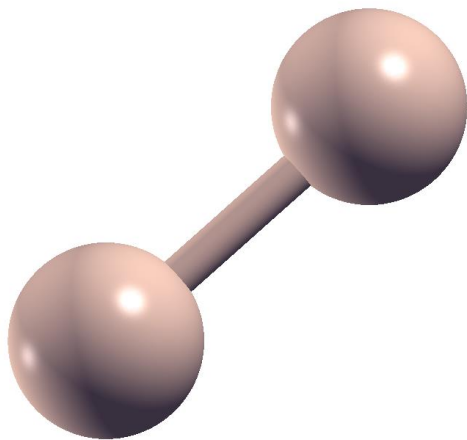


Figure 1(a): Pristine Silicene

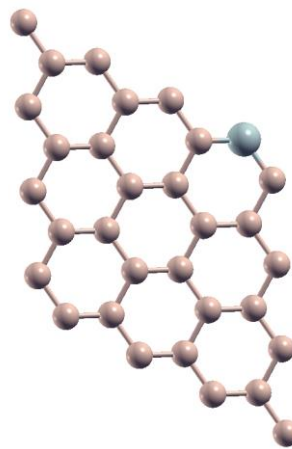


Figure 1(b): Mg:Si = 1:31; 3.125% doping

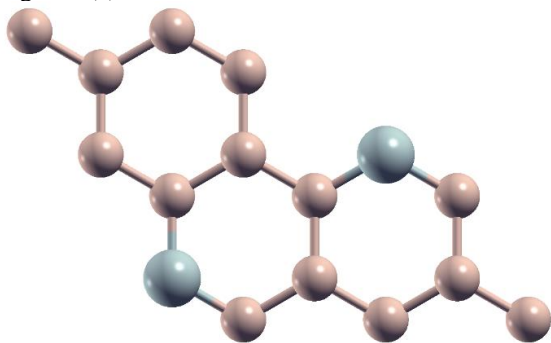


Figure 1(c): Mg:Si = 2:14; 12.5% doping

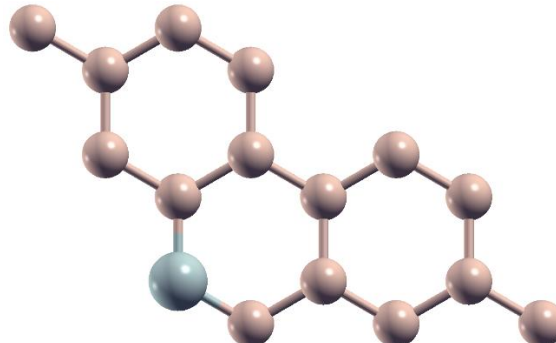


Figure 1(d): Mg:Si = 1:15; 6.25% doping

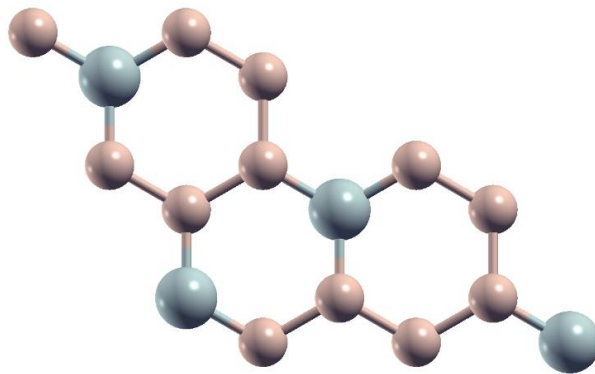


Figure 1(e): Mg:Si = 4:31; 25% doping

### Kinetic Energy Cut-Off (Ecutwfc) Optimization

The kinetic energy cut-off is used to truncate plane waves in the wavefunction expansion for accuracy and computational cost (Poggetto et al., 2020). In a periodic system, the wavefunction for an electron within a plane wave basis set is given by:

$$\psi_k(r) = \frac{1}{\sqrt{\Omega}} \sum_G C_k G e^{i(k+G).r}$$

Here:  $k$  is the wave vector,  $G$  is the reciprocal lattice vector and  $\Omega$  is the volume of the unit cell. The cut-off energy is defined by the condition,

$$\frac{\hbar^2 |k + G|^2}{2m} \leq E_{cut}$$

The above would allow this calculation to involve only plane waves with kinetic energy less than or equal to Ecutwfc. More precise values can be obtained using higher Ecutwfc, but simulations take longer to converge.

### Optimization Process

We used Ecutwfc values ranging from 20 Ry to 300 Ry for Mg-doped silicene, determining what value is needed to achieve convergence of the results. This parameter is tuneable, and the best value depends upon Mg doping levels since, above a certain level, extra structure modifications may be introduced, which could need higher energy cutoffs to simulate accurately.

### K-point Grid Optimization

Ideally, total energy and density calculations require integration over all k-points in the Brillouin zone (BZ) (Jorgensen et al., 2021). However, the integration is performed over a finite number of k-points to make these calculations computationally feasible.

We used the Monkhorst-Pack scheme to define the k-point grid, which specifies the mesh size along each crystallographic direction  $k_1 \times k_2 \times k_3$ . A series of k-point grids, ranging from  $2 \times 2 \times 1$  to  $30 \times 30 \times 1$ , was tested for all doping levels to determine the optimal mesh that ensures convergence of the total energy. The optimal grid size was determined by systematically increasing the number of k-points. As the grid becomes denser, the

precision of the calculation improves but at the cost of longer computation times. The smallest k-point grid that achieved convergence and a stable total energy value was selected for further calculations.

## RESULTS AND DISCUSSION

### Kinetic Energy Cutoff (Ecutwfc) Optimization

The optimization of the kinetic energy cutoff (Ecutwfc) is fundamental in plane-wave density functional theory (DFT) calculations, as it defines the maximum kinetic energy of the plane waves included in the wavefunction expansion. Adequate selection of Ecutwfc ensures the balance between computational efficiency and numerical precision.

The total energy was calculated for Ecutwfc values ranging from 20 Ry to 300 Ry. The total energy for pristine silicene stabilized at an Ecutwfc value of 60 Ry, with variations in total energy falling below the convergence threshold of  $10^{-4}$  Ry for higher cutoff values. This relatively low cutoff reflects the simplicity of the pristine silicene system, which lacks additional complexity from dopant atoms or associated distortions. The introduction of magnesium doping increased the complexity of the system, requiring higher Ecutwfc values for convergence. Fig.2 (a-e) shows that convergence values varied systematically with doping levels. At 3.125% doping, the system converges at 200 Ry. This higher cutoff compared to pristine silicene reflects the added complexity introduced by a single Mg atom in the supercell. For 6.25% doping, convergence occurs at 150 Ry, showing a slight reduction in the required Ecutwfc. This might indicate a balance between dopant density and the computational representation of the system. At 12.5% doping, convergence increases again to 180 Ry; the higher cutoff is likely due to the cumulative effects of charge redistribution and localized distortions around multiple dopant atoms. At 25% doping, the required Ecutwfc reaches 190 Ry, reflecting the significant perturbation introduced by replacing one-quarter of the silicon atoms with magnesium.

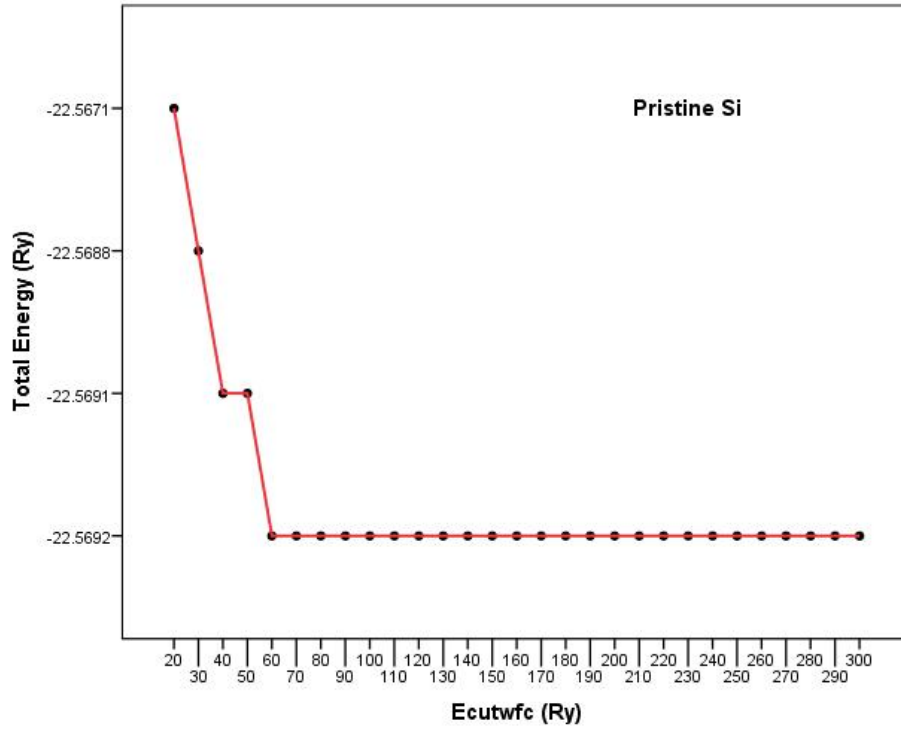


Figure 2(a): Ecutwfc optimization for Pristine Silicene

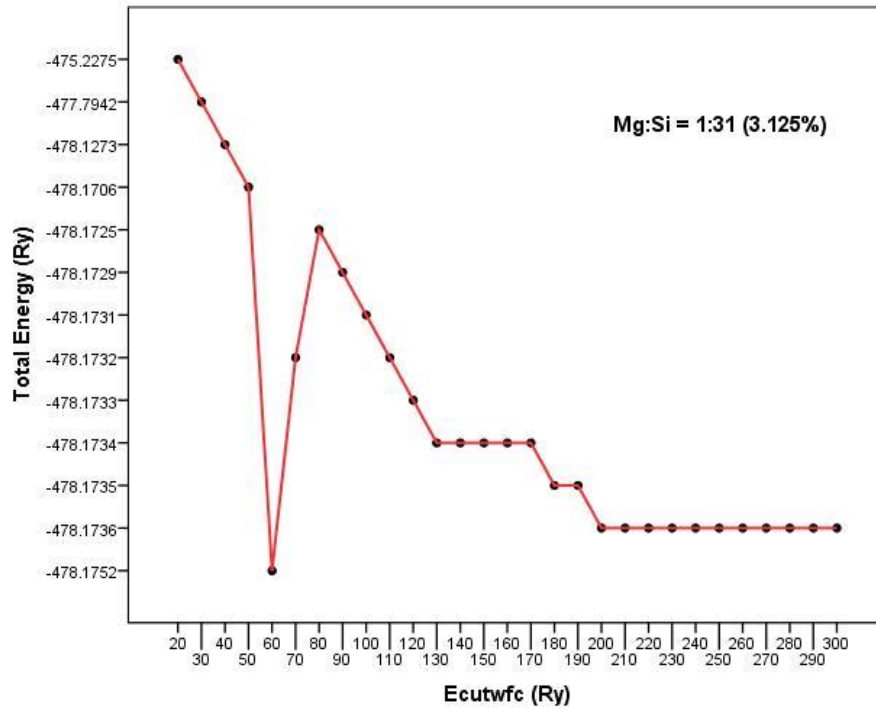


Figure 2(b): Ecutwfc optimization for 3.125% Mg-doped Silicene

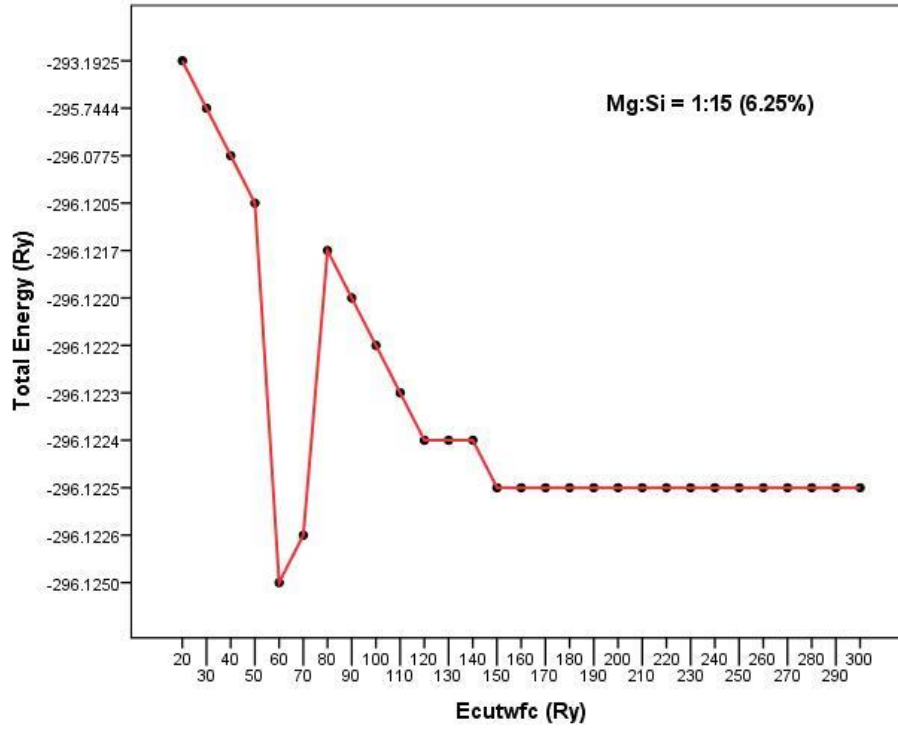


Figure 2(c): Ecutwfc optimization for 6.25% Mg-doped Silicene

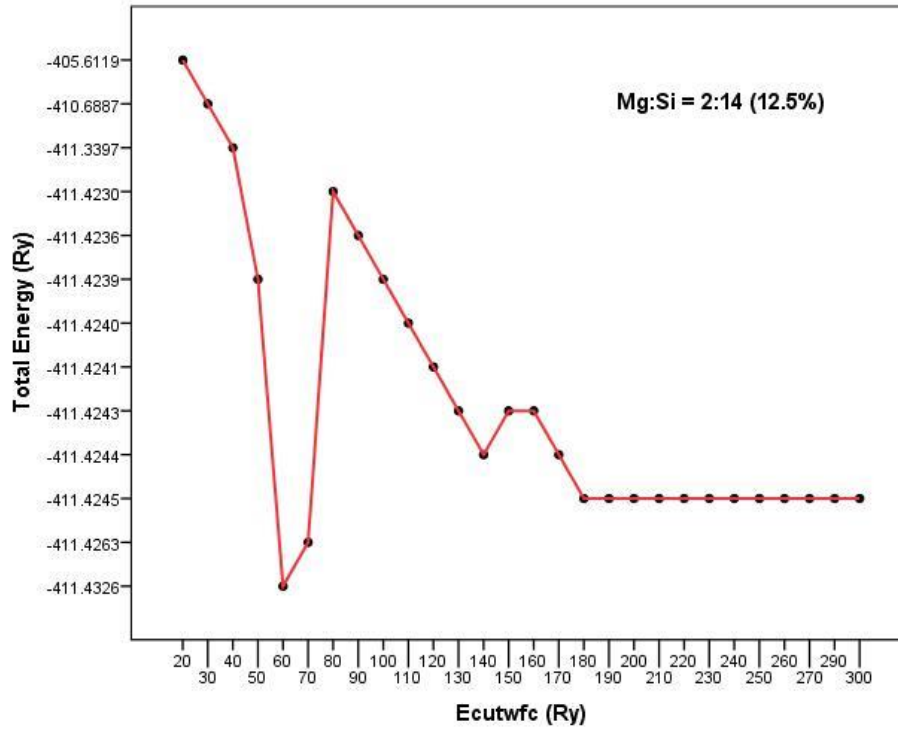


Figure 2(d): Ecutwfc optimization for 12.5% Mg-doped Silicene

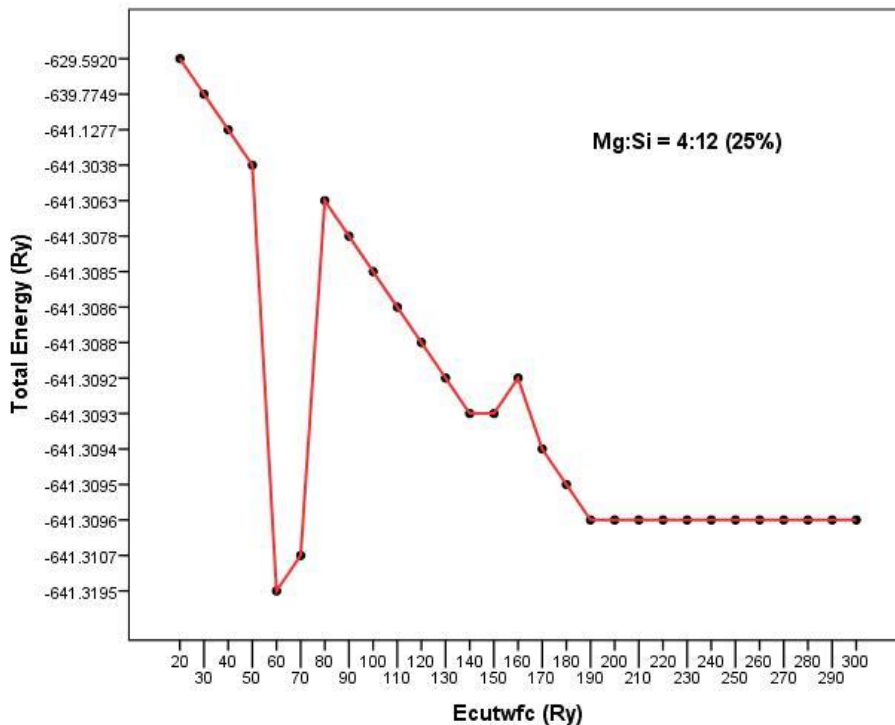


Figure 2(e): Ecutwfc optimization for 25% Mg-doped Silicene

For pristine silicene, the system's total energy stabilized quickly with increasing Ecutwfc, demonstrating that the simpler electronic structure of the undoped material can be effectively captured with a relatively low kinetic energy cutoff. This result aligns with the expectations for pure, planar silicene, where minimal electron-ion interactions and a lack of dopant-induced distortions reduce the need for extensive plane-wave expansion.

In contrast, Mg-doped silicene required significantly higher Ecutwfc values for convergence, varying by doping level. This increase could be attributed to Dopant-Induced Perturbations since the introduction of magnesium atoms modifies the local electronic environment of the silicene lattice, introducing

additional electron-ion interactions and demanding a more extensive plane-wave basis set to achieve numerical accuracy. Higher doping levels exacerbate these perturbations, as the increased number of dopants further disrupts the symmetry and increases the system's electronic complexity.

Magnesium doping leads to significant charge transfer between Mg atoms and surrounding silicon atoms, particularly at higher doping levels. Accurately resolving this redistribution requires a higher kinetic energy cutoff to include the necessary plane waves. Doping can also cause slight lattice distortions, which, though limited in silicene, still require higher Ecutwfc values to capture accurately.

**Table 1: Total energy of Ecutwfc convergence for different doping levels**

Doping Level (%)	Ecutwfc (Ry)	Total Energy
Pristine	60	-22.56920067
3.125	200	-478.17363176
6.25	150	-295.06812945
12.5	180	-411.42451426
25	190	-641.30964200

Table 1 shows a clear trend influenced by doping levels. The total energy of pristine silicene is relatively low at -22.5692 Ry due to the high symmetry and simple electronic structure of the undoped material. However, the introduction of magnesium doping drastically alters the system's electronic environment, leading to

significantly more negative total energy values. As the doping level increases, the total energy becomes progressively more negative, indicating enhanced system stability due to the increased interaction between magnesium atoms and the silicene lattice. The 3.125% doping level has a total energy of -478.1736 Ry, much

lower than the pristine silicene, reflecting the structural and electronic modifications introduced by the single Mg atom substitution. Similarly, for 6.25%, 12.5%, and 25% doping levels, the total energy further decreases to -295.0681 Ry, -411.4245 Ry, and -641.3096 Ry, respectively, showing a consistent relationship between doping concentration and system stabilization. This trend can be attributed to the increasing number of Mg atoms contributing to the bonding interactions within the lattice. Higher doping concentrations lead to greater redistribution of charge density and stronger binding interactions, contributing to the lower total energy; this is in agreement with what Cao et al. (2022) reports. However, the larger distortions and structural perturbations at higher doping levels necessitate higher Ecutwfc values for convergence to capture the modified electronic structure accurately. These results emphasize the significant impact of doping on the overall stability and electronic properties of silicene. The substantial reduction in total energy with increasing doping concentrations suggests that Mg doping can effectively

stabilize silicene, making it a promising candidate for applications in nanoelectronics and energy-related technologies.

**K-Point Grid Optimization**

The convergence of the k-point grid was evaluated for pristine and Mg-doped silicene using the Monkhorst-Pack scheme. Total energy calculations were performed for grids ranging from 2×2×1 to 30×30×1. For pristine silicene, a grid of 14×14×1 was sufficient to achieve convergence, with total energy changes below the 10<sup>-4</sup> Ry tolerance threshold. Similarly, for Mg-doped silicene, the convergence points for the k-point grid were found to be 5×5×1 for 3.125%, 15×15×1 for 6.25%, 16×16×1 for 12.5% and 17×17×1 for 25% as shown in fig.3(a-e). For pristine silicene, a 14×14×1 grid was adequate to ensure convergence. This reflects the periodicity and simplicity of the pristine structure, where a moderately dense k-point sampling is sufficient to capture the electronic properties accurately.

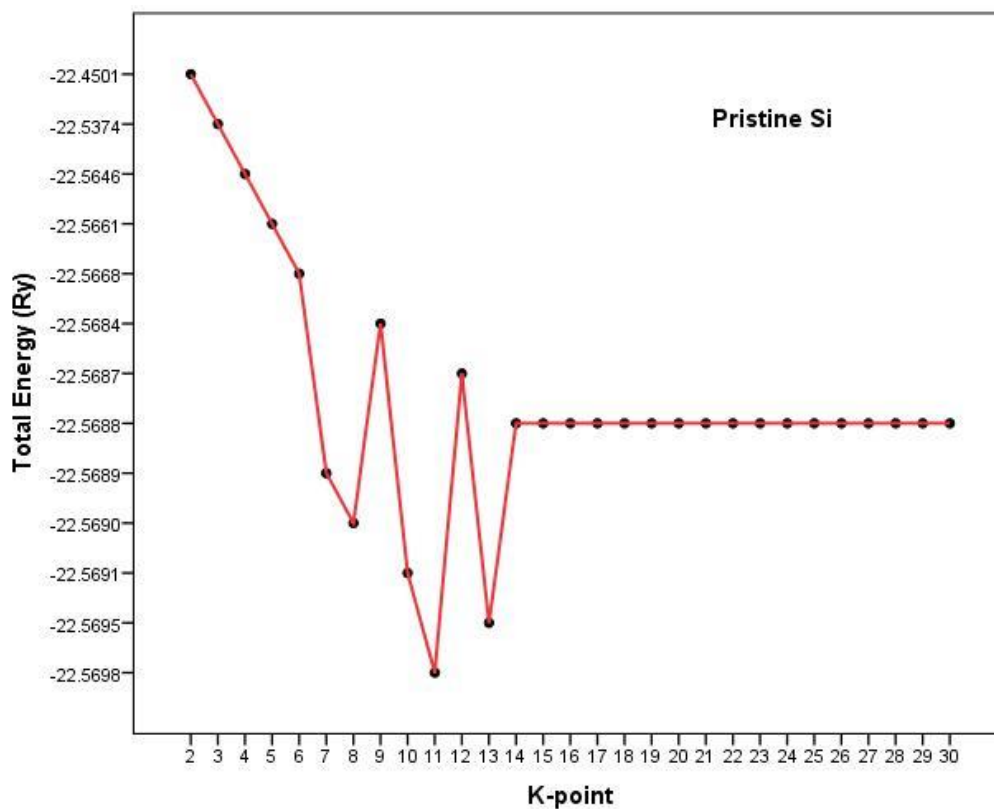


Figure 3(a): K-point Grid optimization for Pristine Silicene

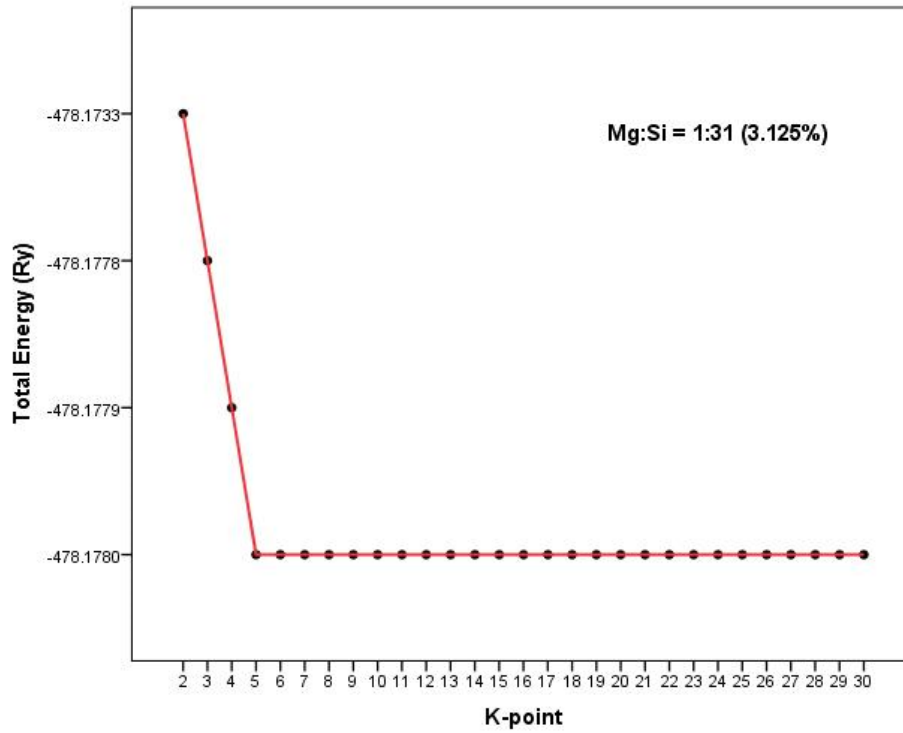


Figure 3(b): K-point Grid optimization for 3.125% Mg-doped Silicene

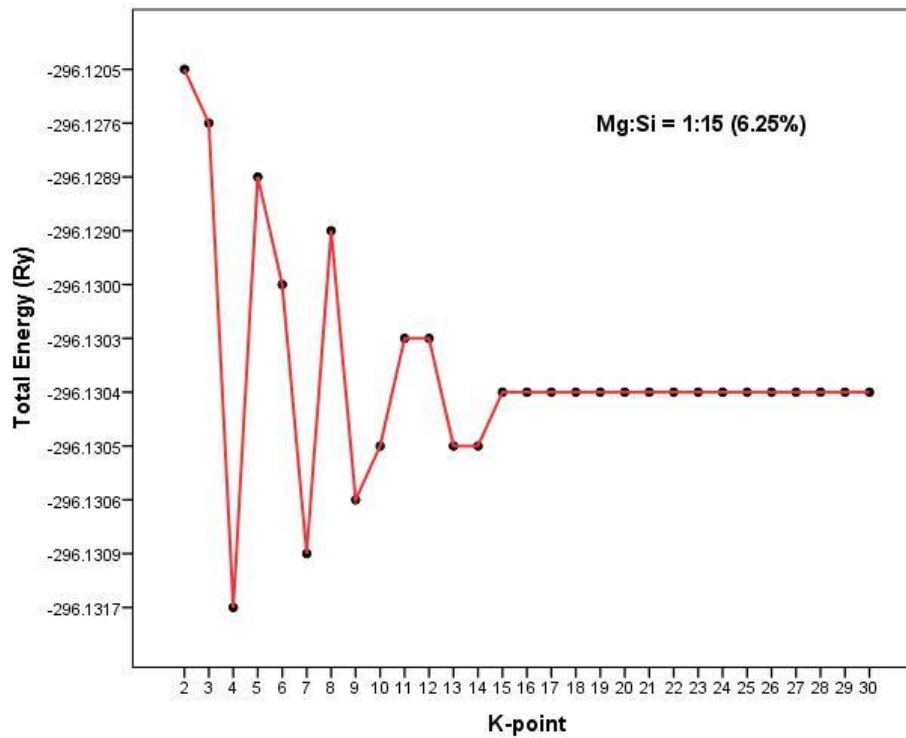


Figure 3(c): K-point Grid optimization for 6.25% Mg-doped Silicene



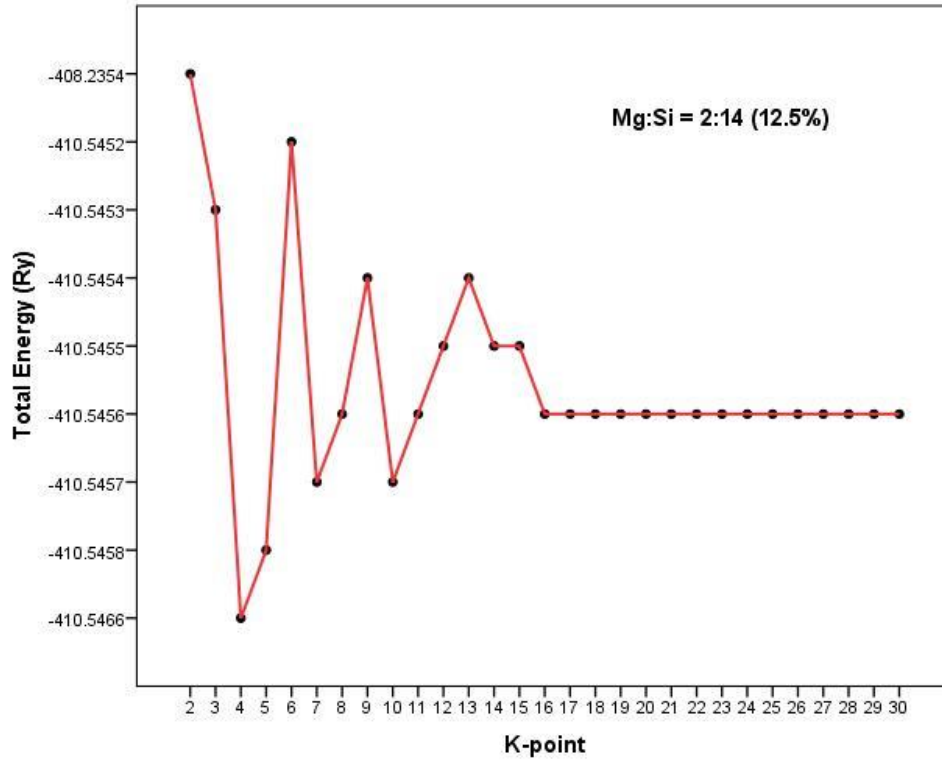


Figure 3(d): K-point Grid optimization for 12.5% Mg-doped Silicene

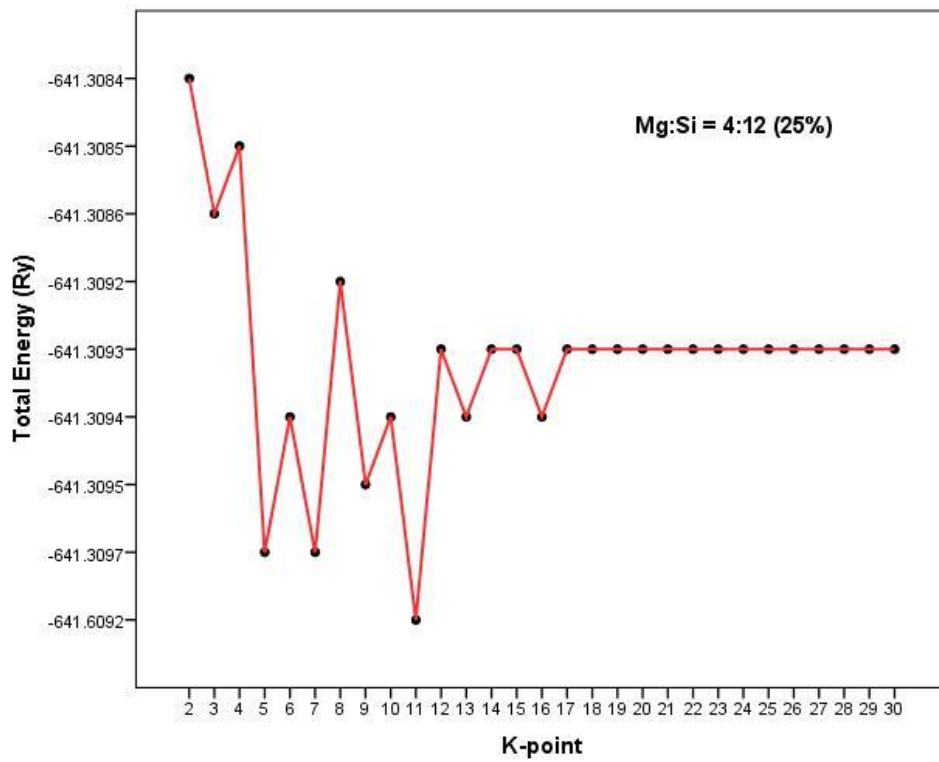


Figure 3(e): K-point Grid optimization for 25% Mg-doped Silicene

In the case of Mg-doped silicene, the convergence grid became increasingly fine with higher doping concentrations as 3.125% doping converged with a  $5 \times 5 \times 1$  grid. The magnesium atoms introduce only minor perturbations to the silicene lattice and electronic structure at this very low doping level. These perturbations do not significantly increase the complexity of the electronic interactions, and a coarser k-point grid is sufficient to achieve convergence—the lower doping results in localized electronic effects that are easier to resolve without dense sampling. As the doping concentration increases, with 6.25%, 12.5%, and 25%, the electronic structure becomes more complex due to stronger interactions between the dopant atoms

and the silicene lattice. These interactions result in a more intricate Brillouin zone, necessitating finer k-point grids to resolve the energy bands and total energy changes accurately.

The total energy results for pristine silicene and Mg-doped silicene systems, calculated at their respective converged k-point grids, provide critical insights into the impact of doping on the electronic structure and system stability. Pristine silicene had a total energy of -22.5688 Ry, reflecting the simple electronic structure and high symmetry of the undoped material. The required k-point grid for convergence ( $14 \times 14 \times 1$ ) is moderately dense, ensuring accurate sampling of the Brillouin zone for this pristine system.

**Table 2: Total energy of k-point convergence for different doping levels**

Doping Level (%)	K-point Grid	Total Energy (Ry)
Pristine	$14 \times 14 \times 1$	-22.56877491
3.125	$5 \times 5 \times 1$	-478.17804218
6.25	$15 \times 15 \times 1$	-296.132535334
12.5	$16 \times 16 \times 1$	-411.43317668
25	$17 \times 17 \times 1$	-641.30939814

As shown in Table 2, magnesium doping significantly reduces total energy, indicating increased system stability due to the stronger interactions within the doped lattice. For the 3.125% doping level, the total energy drops to -478.1780 Ry. Interestingly, this low doping concentration requires only a coarse k-point grid ( $5 \times 5 \times 1$ ) for convergence, likely due to the localized effects of a single Mg atom substitution in a relatively large supercell.

As the doping concentration increases, the total energy decreases, reaching -296.1325 Ry for 6.25%, -411.4332 Ry for 12.5%, and -641.3094 Ry for 25%. This consistent trend toward more negative total energy values underscores the stabilizing effect of higher Mg concentrations, which enhance the bonding interactions and modify the electronic structure. However, the increasing doping levels also introduce greater electronic complexity, necessitating finer k-point grids for accurate sampling. The k-point grids required for convergence increase progressively to  $15 \times 15 \times 1$ ,  $16 \times 16 \times 1$ , and  $17 \times 17 \times 1$  for the 6.25%, 12.5%, and 25% doping levels, respectively. This result is similar to that of Gidado, et al (2024) who obtained a k-point grid of  $15 \times 15 \times 1$  for 8-atom silicene.

Doping introduces symmetry-breaking effects in the silicene lattice; at very low doping levels, these effects are localized and do not drastically alter the overall symmetry of the system, allowing for coarser grids. As the doping concentration increases, the symmetry-breaking effects propagate throughout the lattice, creating more intricate features in the electronic structure. This reduces the symmetry of the Brillouin zone, requiring finer k-point meshes for accurate

calculations. These results illustrate the dual effect of Mg doping on silicene: it enhances stability, as evidenced by the more negative total energy, but also increases computational demands due to the need for finer k-point grids to capture the complex electronic interactions. This relationship shows the importance of optimizing computational parameters to accurately describe doped systems, providing a robust framework for exploring the properties of Mg-doped silicene for potential applications in nanoelectronics and energy storage devices.

## CONCLUSION

The convergence behaviour of Ecutwfc and k-point grid across doping levels highlights the interplay between structural and electronic modifications introduced by Mg doping. Doping consistently increases the Ecutwfc requirement compared to pristine silicene due to the need to capture the localized effects of Mg atoms and the additional electronic states they introduce. For instance, pristine silicene converges at 60 Ry with a total energy of -22.5692 Ry, while the highest Ecutwfc (200 Ry) is observed for 3.125% doping, which achieves a total energy of -478.1736 Ry. Other doping levels, such as 6.25%, 12.5%, and 25%, converge at 150 Ry, 180 Ry, and 190 Ry, respectively, with total energies of -295.0681 Ry, -411.4245 Ry, and -641.3096 Ry, indicating the increasing stability of the system with higher Mg concentrations. In contrast, the k-point grid convergence behaves nonlinearly across doping levels. The 3.125% doping level requires the coarsest grid ( $5 \times 5 \times 1$ ) due to the localized and minimal impact of Mg atoms on the electronic structure despite its significantly

lower total energy compared to pristine silicene. As doping increases, the k-point grid requirements rise steadily, reflecting the increasing complexity and delocalization of the electronic states across the Brillouin zone. For 6.25%, 12.5%, and 25% doping levels, convergence is achieved at  $15 \times 15 \times 1$ ,  $16 \times 16 \times 1$ , and  $17 \times 17 \times 1$ , respectively, with corresponding total energies of  $-296.1325$  Ry,  $-411.4332$  Ry, and  $-641.3094$  Ry. This study underscores optimizing computational parameters to balance accuracy and efficiency. Tailoring Ecutwfc and k-point grids to specific doping concentrations provides a benchmark for future theoretical investigations of Mg-doped silicene systems. The observed trends in total energy further emphasize the stabilizing effects of doping, offering valuable insights for accurately modelling Mg-doped silicene and similar 2D materials, paving the way for practical applications in nanoelectronics, energy storage, and optoelectronic devices.

#### ACKNOWLEDGEMENT

We acknowledge Common Infrastructure for National Cohorts in Europe, Canada, and Africa (CINECA) for access to Leonardo and Galileo100 supercomputing hosted at CINECA, Italy.

#### REFERENCES

Adelaja, A. D., Onma, O. S., Idowu, B. A., Opeifa, S. T., & Ogabi, C. O. (2024). Jerk Chaotic System: Analysis, Circuit Simulation, Control and Synchronization with Application to Secure Communication. *Nigerian Journal of Theoretical and Environmental Physics*, 2(2), 56-69.

Babbush, R., Wiebe, N., McClean, J., McClain, J., Neven, H., & Chan, G. (2017). Low-Depth Quantum Simulation of Materials. *Physical Review X*, 8, 011044. <https://doi.org/10.1103/PhysRevX.8.011044>.

Cao, T., Ren, G., Shao, D., Tsymbal, E., & Mishra, R. (2022). Stabilizing polar phases in binary metal oxides by hole doping. *PHYSICAL REVIEW MATERIALS*. <https://doi.org/10.1103/physrevmaterials.7.044412>

Choudhary, K., & Tavazza, F. (2018). Convergence and machine learning predictions of Monkhorst-Pack k-points and plane-wave cut-off in high-throughput DFT calculations. *Computational materials science*, 161. <https://doi.org/10.1016/j.commatsci.2019.02.006>.

Chowdhury, S., & Jana, D. (2016). A theoretical review on electronic, magnetic and optical properties of silicene. *Reports on Progress in Physics*, 79. <https://doi.org/10.1088/0034-4885/79/12/126501>.

Cocoletzi, H., & Águila, J. (2017). DFT studies on the Al, B, and P doping of silicene. *Superlattices and Microstructures*, 114, 242-250. <https://doi.org/10.1016/J.SPMI.2017.12.040>.

Feng, J., Liu, Y., Wang, H., Zhao, J., Cai, Q., & Wang, X. (2014). Gas adsorption on silicene: A theoretical study. *Computational Materials Science*, 87, 218-226. <https://doi.org/10.1016/J.COMMATSCI.2014.02.025>.

François Gygi (2023). All-Electron Plane-Wave Electronic Structure Calculations. *Journal of Chemical Theory and Computation* 2023 19 (4), 1300-1309 <https://doi.org/10.1021/acs.jctc.2c01191>

Prandini, G., Marrazzo, A., Castelli I. E., Mounet N., and Marzari N., *npj Computational Materials* 4,72 (2018).  
WEB: <http://materialscloud.org/sssp>.

Galashev, A. (2024). Prospects for using silicene as an anode for lithium-ion batteries. A review. *Journal of Energy Storage*, 93, 112281. <https://doi.org/10.1016/j.est.2024.112281>

Galashev, A., & Vorob'ev, A. (2023). Ab Initio Study of the Electronic Properties of a Silicene Anode Subjected to Transmutation Doping. *International Journal of Molecular Sciences*, 24. <https://doi.org/10.3390/ijms24032864>.

Gheshlagh, Z., Beheshtian, J., & Mansouri, S. (2020). The electronic and optical properties of 3d transition metals doped silicene sheet: A DFT study. *Materials Research Express*, 6. <https://doi.org/10.1088/2053-1591/ab6541>.

Gidado, A., Solomon, R., Abubakar, L., Ahmed, F., & Haladu, S. (2024). First Principle Investigations of Structural, Electronic and Thermal Properties of Pristine, Metal and Non-Metal Doped Silicene for Thermoelectric Applications. *PHYSICS ACCESS*. <https://doi.org/10.47514/phyaccess.2024.4.2.010>.

Jorgensen, J. & Christensen, J. & Jarvis, Tyler & Hart, Gus. (2021). A general algorithm for calculating irreducible Brillouin zones. 10.48550/arXiv.2104.05856.

Kokalj, A. (1999) XCrySDen—A New Program for Displaying Crystalline Structures and Electron Densities. *Journal of Molecular Graphics and Modelling*, 17, 176-179. <http://www.xcrysden.org/>

Mg. Pbesol-rrkjus\_psl.1.0.0.UPF, from *Pslibrary 1.0.0*: A. Dal Corso, *Comput. Mater. Sci.* 95, 337 (2014).

<http://dx.doi.org/10.1016/j.commatsci.2014.07.043>

<http://www.quantum-espresso.org/pseudopotentials>,

LICENSE: GNU General Public License (version 2 or later).

Ornes, S. (2014). Silicene. Proceedings of the National Academy of Sciences, 111(30), 10899. <https://doi.org/10.1073/pnas.1410332111>

Giannozzi, P., Andreussi O., Brumme T., Bunau O., Buongiorno M., Nardelli, Calandra M., Car R., Cavazzoni C., Ceresoli D., Cococcioni M., Colonna N., Carnimeo I., Dal Corso A., de Gironcoli S., Delugas P., DiStasio Jr R A., Ferretti A., Floris A., Fratesi G., Fugallo G., Gebauer R., Gerstmann U., Giustino F., Gorni T., Jia J., Kawamura M., Ko H-Y., Kokalj A., Küçükbenli E., Lazzeri M., Marsili M., Marzari N., Mauri F., Nguyen N L., Nguyen H-V., Otero-de-la-Roza A., Paulatto L., Poncé S., Rocca D., Sabatini R., Santra B., Schlipf M., Seitsonen A P., Smogunov A., Timrov I., Thonhauser T., Umari P., Vast N., Wu X and Baroni S, *J.Phys.:Condens.Matter* **29**, 465901 (2017) <https://doi.org/10.1088/1361-648X/aa8f79>

. Giannozzi P, Baseggio O., Bonfà P., Brunato D., Car R., Carnimeo I., Cavazzoni C., de Gironcoli S., Delugas P., Ferrari Ruffino F., Ferretti A., Marzari N., Timrov I., Urru A., Baroni S. ; *J. Chem. Phys.* 152, 154105 (2020)  
Giannozzi P., Baroni S., Bonini N., Calandra M., Car R., Cavazzoni C., Ceresoli D., Chiarotti G. L., Cococcioni M., Dabo I., Dal Corso A., Fabris S., Fratesi G., de Gironcoli S., Gebauer R., Gerstmann U., Gougoussis C., Kokalj A., Lazzeri M., Martin-Samos L., Marzari N., Mauri F., Mazzarello R., Paolini S., Pasquarello A., Paulatto L., Sbraccia C., Scandolo S., Sclauzero G., Seitsonen A. P., Smogunov A., Umari P., Wentzcovitch R. M., *J. Phys. Condens. Matter* **21**, 395502 (2009) <http://iopscience.iop.org/0953-8984/21/39/395502/>

Poggetto, V., & Serpa, A. (2020). Elastic wave band gaps in a three-dimensional periodic metamaterial using

the plane wave expansion method. *International Journal of Mechanical Sciences*, 184, 105841. <https://doi.org/10.1016/j.ijmecsci.2020.105841>.

Si.pbesol-n-rrkjus\_psl.1.0.0.UPF, from Pslibrary 1.0.0: A. Dal Corso, *Comput. Mater. Sci.* 95, 337 (2014). <http://dx.doi.org/10.1016/j.commatsci.2014.07.043>, <http://www.quantum-espresso.org/pseudopotentials>, LICENSE: GNU General Public License (version 2 or later).

Sun, W., Li, L., Zhang, J., & Yin, H. (2018). Theoretical Study of Phonon Dispersion of Lanthanum Aluminate in Terahertz Frequency., 90-96. <https://doi.org/10.1016/j.procs.2019.01.196>.

Tran NTT, Gumbs G, Nguyen DK, Lin MF. Fundamental Properties of Metal-Adsorbed Silicene: A DFT Study. *ACS Omega*. 2020 Jun 4;5(23):13760-13769. doi: 10.1021/acsomega.0c00905. PMID: 32566841; PMCID: PMC7301544.

Tran, F. & Blaha, P. (2017). Importance of the Kinetic Energy Density for Band Gap Calculations in Solids with Density Functional Theory. *The Journal of Physical Chemistry* 121 (17), 3318-3325 <https://doi.org/10.1021/acs.jpca.7b02882>

Uwaoma, C. J., Oriaku, C. I., Joseph, U. and Nnanna, L.A, (2024). Theoretical Study of Exciton Properties of Dilute GaInAsN Semiconductors. *Nigerian Journal of Theoretical and Environmental Physics (NJTEP)* ISSN Print: 3026-9601 DOI: <https://doi.org/10.62292/njtep.v2i2.2024.52> Volume 2(2)

Zhao, J., Liu, H., Yu, Z., Quhe, R., Zhou, S., Wang, Y., Liu, C., Zhong, H., Han, N., Lu, J., Yao, Y., & Wu, K. (2016). Rise of silicene: A competitive 2D material. *Progress in Materials Science*, 83, 24-151. <https://doi.org/10.1016/J.PMATSCI.2016.04.001>.